THEORETICAL STUDY OF A MODEL FOR THE ATP CAP AT THE END OF AN ACTIN FILAMENT

TERRELL L. HILL
Laboratory of Molecular Biology, National Institute of Arthritis, Diabetes, and Digestive and Kidney Diseases, National Institutes of Health, Bethesda, Maryland 20205

ABSTRACT The model used successfully by Pantaloni et al. to fit experimental data on steady-state actin polymerization is investigated theoretically. Many properties are deduced, as functions of the free subunit concentration. The model is simple enough so that one can examine analytically the question of whether actin shows the same dramatic phase changes associated with the GTP cap in microtubules. The answer is negative, judging from this model. However, it is possible to obtain such phase changes using the same model but with quite different, hypothetical choices of parameters. Thus, aside from its application to actin, this model is useful pedagogically to illustrate the nature of phase changes that may occur at the end of a steady-state polymer.

A new model for actin polymerization has been applied to experimental data in a recent paper (1). The theoretical analysis of the model in reference 1 is extended considerably here. In particular, the model is simple enough so that it is possible to investigate analytically the possibility of phase changes at an end of an actin filament, associated with the presence or absence of an ATP cap. The situation is found to be quite different than for an end of a microtubule (2–5).

THE MODEL AND ITS PROPERTIES

The model is explained in detail in reference 1. A brief summary is given here. One end (denoted α) of an actin filament, say the more active "barbed" end, is shown schematically in Fig. 1 *A*. T represents a subunit of ATP-actin, D an ADP-actin subunit. It is assumed that the interior of the filament is all D and that there are $N = 0, 1, 2 \ldots$ consecutive T's at the tip (N is the size of the ATP cap). This simple configuration arises because the solution contains (by assumption) a significant concentration (c) of free T subunits only, and ATP hydrolysis (rate constant k_H), converting T to D, can occur only at the boundary between T's and D's (e.g., in Fig. 1 *A*, at position $n = N = 4$ only). This oversimplification in the model is what makes the analysis, given below, possible. This model is rather similar to the microtubule model introduced in the appendix of Carlier et al. (6).

The kinetic diagram is presented in Fig. 1 *B*. The state $N = 0$ is the polymer DDD . . . , with no cap. In this diagram, we follow the size of the ATP cap, not the size of the polymer itself. The attachment rate constants for T's are denoted k_1, k_2, and k_3 (for $N \geq 2$) and the detachment rate constants, for T's are k_{-1}, k_{-2}, and k_{-3} (for $N \geq 3$). Hydrolysis can occur only at the boundary position $n = N$, and only then if $N \geq 3$ (i.e., a T at $n = 1$ or $n = 2$ can never hydrolyze). Attachment equilibrium constants are designated $K_i = k_i/k_{-i}$ $(i = 1, 2, 3)$.

The rate constant for loss of D from the tip of the uncapped polymer $N = 0$ is denoted k_{-D}. This rate constant does not appear in Fig. 1 *B* because state $N = 0$ remains in the same state when a D is lost.

Because the kinetic diagram in Fig. 1 *B* is linear, the steady-state distribution of polymer α ends among states $N = 0, 1, 2 \ldots$ follows a "detailed balance" solution (7):

$$k_1 c p_0 = k_{-1} p_1,\ k_2 c p_1 = k_{-2} p_2,\ k_3 c p_2 = (k_{-3} + k_H) p_3, \quad (1)$$

etc., where p_N is the probability that a polymer α end is in state N (has a cap of size N). The normalized p_N are then easy to find:

$$p_0 = (1 - x)/D, \quad p_1 = (1 - x)K_1 c/D,$$
$$p_N = (1 - x)K_1 K_2 c^2 x^{N-2}/D \qquad (N \geq 2), \quad (2)$$

where

$$x = k_3 c/(k_{-3} + k_H),\ D \equiv (1 - x)(1 + K_1 c) + K_1 K_2 c^2. \quad (3)$$

It should be noted that x is proportional to c. The p_N in Eq. 2 converge provided that $x < 1$, that is, provided that $c < c_0$, where the transition concentration c_0 is given by

$$c_0 \equiv (k_{-3} + k_H)/k_3. \quad (4)$$

Thus, x can also be written as c/c_0. The regime $c > c_0$ is discussed separately, below.

The probability that the cap has $N \geq 3$ (hence, hydrolysis can occur) is

$$f_I = 1 - p_0 - p_1 - p_2 = xK_1 K_2 c^2/D. \quad (5)$$

The subscript I refers to phase I, introduced later. When $x \to 1$, i.e., when $c \to c_0$, $f_I \to 1$.

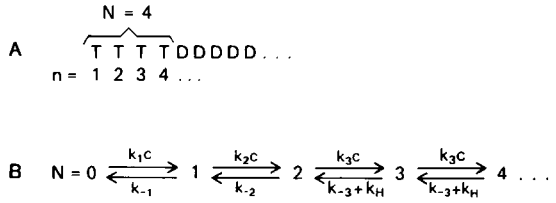

FIGURE 1 (*a*) Illustrative configuration at one end (say, α) of an actin filament. T is ATP · actin, D is ADP · actin. N is the number of T's in the ATP cap, n specifies the positions of the α end subunits in the polymer. (*b*) Kinetic diagram, with rate constants, that relates various values of N.

The mean size of the cap is found to be

$$\bar{N} = \sum_{N=0}^{\infty} N p_N = K_1 c[(1-x)^2 + K_2 c(2-x)]/(1-x)D. \quad (6)$$

When $x \to 1$, $\bar{N} \to \infty$. Also the variance in N, relative to $\bar{N}^2$, is

$$\frac{\sigma^2}{\bar{N}^2} = \frac{(1-x)^4 + K_2 c(1-x)(4-3x+x^2) + K_1 K_2 c^2(1-x^2) + K_1 K_2^2 c^3 x}{K_1 c[(1-x)^2 + K_2 c(2-x)]^2} \quad (7)$$

where $\sigma^2 \equiv \overline{N^2} - \bar{N}^2$.

Let P_n be the probability that position n has a T. Then

$$P_n = p_n + p_{n+1} + \cdots, \quad (8)$$

$$P_1 = 1 - p_0,\ P_2 = 1 - p_0 - p_1,$$

$$P_3 = 1 - p_0 - p_1 - p_2 = f_1, \quad (9)$$

$$P_n = K_1 K_2 c^2 x^{n-2}/\mathrm{D} \qquad (n \geq 2), \quad (10)$$

$$\bar{N} = P_1 + P_2 + P_3 + \cdots. \quad (11)$$

Eqs. 6 and 11 are alternative ways of expressing $\bar{N}$.

The steady-state subunit flux per polymer α end is, from Fig. 1 *B*,

$$J = -k_{-D}p_0 + (k_1 c p_0 - k_{-1}p_1) + (k_2 c p_1 - k_{-2}p_2) + (k_3 c p_2 - k_{-3}p_3) + \cdots. \quad (12)$$

Because of the steady-state "detailed balance" relations in Eq. 1, the first two expressions in parenthesis in Eq. 12 are zero, the third is $k_H p_3$, etc. Hence

$$J = -k_{-D}p_0 + J_H, \quad J_H = k_H f_1. \quad (13)$$

Here J_H is the rate of hydrolysis of ATP per α end. At steady state, the net mean rate at which T subunits enter the α end via on and off transitions (Eq. 12) must equal the net mean rate J_H at which T subunits disappear by hydrolysis (Eq. 13).

The mean cap size $\bar{N} \to \infty$ as $c \to c_0$. For $c > c_0$, the cap is always present but has no definite mean size: it increases steadily with time. The hydrolysis rate in this case is $J_H = k_H$, a constant, and the net rate at which subunits are added to the polymer is $J = k_3 c - k_{-3}$. The steady rate at which the cap grows is then $J - J_H > 0$. At $c = c_0$, the $c < c_0$ regime and the $c > c_0$ regime have the same properties:

$$J = J_H = k_H = k_3 c_0 - k_{-3}. \quad (14)$$

There is a discontinuity in the slope of $J(c)$ and of $J_H(c)$ at $c = c_0$. For $c \geq c_0$, $J_H'(c) = k_3$ and $J_H'(c) = 0$. For the lower branches ($c \leq c_0$) of J and J_H,

$$J'(c_0) = k_{-D}(K_1 K_2 c_0^3)^{-1} + J_H'(c_0), \quad (15)$$

$$J_H'(c_0) = k_H c_0^{-1}[1 + (K_2 c_0)^{-1} + (K_1 K_2 c_0^2)^{-1}]. \quad (16)$$

Also, at $c = 0$, the slopes are

$$J'(0) = k_{-D}K_1, \quad J_H'(0) = 0. \quad (17)$$

We denote the value of c at which $J = 0$ by $c = c_\alpha$ (the critical concentration of the α end). Then the cubic equation that determines c_α follows from Eq. 13:

$$k_{-D}[1 - (c_\alpha/c_0)] = k_H K_1 K_2 c_\alpha^3/c_0. \quad (18)$$

Fig. 2 illustrates some of the above features in the same case used in reference 1 to fit experimental data: $K_1 = 1.5196\ \mu\mathrm{M}^{-1}$, $K_2 = 15.196\ \mu\mathrm{M}^{-1}$, $k_H = 13.6\ \mathrm{s}^{-1}$, $k_{-D} = 5\ \mathrm{s}^{-1}$, $k_3 = 1.7\ \mu\mathrm{M}^{-1}\ \mathrm{s}^{-1}$, and $k_{-3} = 5.1\ \mathrm{s}^{-1}$. These parameters give $c_0 = 11\ \mu\mathrm{M}$ and $c_\alpha = 0.55\ \mu\mathrm{M}$. A large mean cap ($\bar{N}$) is attained only when c approaches c_0. The fluctuations (σ^2) in cap size are also large in this region because $\sigma^2/\bar{N}^2$ is of order unity.

Fig. 2 exhibits an extensive range in c, $1 \leq c \leq 11\ \mu\mathrm{M}$, in

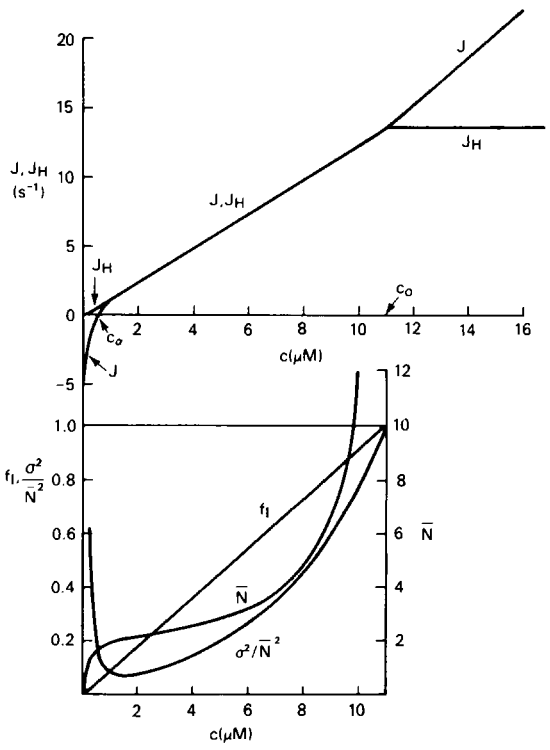

FIGURE 2 Calculated curves, as functions of c, for the same case used in reference 1 to fit experimental $J(c)$ data.

which J, J_H, and f_I behave approximately linearly with c. In this range, approximate simple expressions are

$$p_0 \simeq p_1 \simeq 0, \quad p_2 \simeq 1 - x, \quad f_I \simeq x, \quad J \simeq J_H \simeq k_H x,$$
$$\bar{N} \simeq (2 - x)/(1 - x), \quad \sigma^2/\overline{N^2} \simeq x/(2 - x)^2. \quad (19)$$

DOES THIS MODEL EXHIBIT PHASE CHANGES?

Over a considerable range in concentration, a microtubule end (2–5) alternates infrequently between a slowly growing phase (with a GTP cap) and a rapidly shortening phase (with no GTP cap). Because there are hundreds or thousands of elementary transitions (subunits on or off, GTP hydrolysis, etc.) while in one phase, before a change to the other phase, it is a great simplification, without significant loss of accuracy, to use a "macroscopic" two-phase kinetic scheme in place of the much more detailed original scheme of elementary ("microscopic") transitions (2, 3). The rate constants of the two-phase macroscopic scheme are composites or averages of the rate constants of the microscopic scheme.

In the microtubule case, the microscopic kinetic scheme is sufficiently complicated that it is necessary to use Monte Carlo calculations (2, 3) in order to deduce the corresponding composite rate constants of the macroscopic two-phase kinetic diagram. Once these rate constants are available, many properties of the much simpler two-phase scheme can then be found analytically (8, 9).

The attractive feature of the present elementary or microscopic kinetic model for actin polymerization (Fig. 1) is that it is so simple that the connection between microscopic and macroscopic (two-phase) kinetics can be worked out analytically; a Monte Carlo treatment is not necessary for this purpose (though it has been used in a few cases, with the help of Dr. Yi-der Chen, to confirm analytical results qualitatively).

In this section we establish, first, the formal connection between microscopic and macroscopic kinetics for the model. These results are then applied to the above example of actin polymerization (Fig. 2), with negative results (i.e., the two phase simplication is found to be inappropriate for this example). Finally, a hypothetical special case of Fig. 1 is examined that does show rather clean two-phase behavior. Not surprisingly, this latter, very simple, special case bears some resemblance to microtubule elementary kinetics. Thus, two-phase behavior is found to be implicit in the kinetic scheme of Fig. 1 for some parameter choices but not for others (e.g., actin in Fig. 2).

The upper branches of $J(c)$ and $J_H(c)$ ($c \geq c_0$) in Fig. 2 refer to $N \geq 3$ in Fig. 1 *B*. These functions are separated from the lower branches by discontinuities in slope at $c = c_0$. It is therefore natural, for this model, to define the capped phase I as $N \geq 3$. Hydrolysis of ATP occurs only in phase I (at the rate k_H). The uncapped phase II is then comprised of $N = 0, 1, 2$, of which $N = 1$ and $N = 2$ may be regarded as only incipient ATP caps. At steady-state, the probability of phase I is $f_I = 1 - p_0 - p_1 - p_2$, whereas the probability of phase II is $f_{II} = p_0 + p_1 + p_2$, with $f_I + f_{II} = 1$. These are the p_N introduced in Eqs. 2.

The instantaneous subunit flux per α end, in an ensemble of α ends all in state N, is J_N, where (see Fig. 1 *B*)

$$J_0 = k_1 c - k_{-D}, \quad J_1 = k_2 c - k_{-1}, \quad J_2 = k_3 c - k_{-2},$$
$$J_N = k_3 c - k_{-3} \qquad (N \geq 3). \quad (20)$$

Then J can be written (see Eq. 12) as

$$J = p_0 J_0 + p_1 J_1 + p_2 J_2 + (1 - p_0 - p_1 - p_2) J_3$$
$$= f_{II} J_{II} + f_I J_I, \quad (21)$$

where J_I is the mean flux in phase I and J_{II} is the mean flux in phase II. From Eq. 21,

$$J_I = J_3 = k_3 c - k_{-3}, \quad J_{II} = (p_0 J_0 + p_1 J_1 + p_2 J_2)/f_{II}. \quad (22)$$

Explicitly, from Eqs. 2,

$$J_{II} = [(k_1 c - k_{-D}) + K_1 c(k_2 c - k_{-1}) + K_1 K_2 c^2 (k_3 c - k_{-2})]/\Sigma$$
$$\Sigma \equiv 1 + K_1 c + K_1 K_2 c^2. \quad (23)$$

The successive terms in Σ are the weights for states 0, 1, 2 at steady state.

In phase I, the first-order rate constant for subunit addition is $k_3 c$ (Eq. 22) and for subunit loss is k_{-3}. Similarly, in phase II, we denote the corresponding effective or average on and off rate constants by

$$J_{II} = k_{II} c - k_{-II}, \quad (24)$$

$$k_{II} c = (k_1 + K_1 c \cdot k_2 + K_1 K_2 c^2 \cdot k_3) c/\Sigma, \quad (25)$$

$$k_{-II} = (k_{-D} + K_1 c \cdot k_{-1} + K_1 K_2 c^2 \cdot k_{-2})/\Sigma. \quad (26)$$

These rate constants, functions of c, are averages over states 0, 1, and 2.

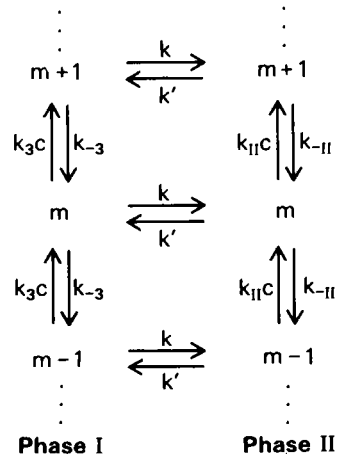

FIGURE 3 Two-phase kinetic diagram. The integer m refers to the number of subunits added to the α end, with arbitrary origin ($m = 0$).

The rate of ATP hydrolysis, J_H, receives no contribution from phase II. Hence $J_H = k_H f_I$ (as in Eq. 13).

Fig. 3 is the two-phase macroscopic kinetic diagram we are in the process of developing. The subunit on and off rate constants for the two phases, just introduced, are included in Fig. 3. Unlike Fig. 1 *B*, the integer m counts subunit gain or loss from the α end, with an arbitrary origin ($m = 0$).

We turn now to the phase change rate constants k and k', which also appear in Fig. 3. At steady state, because k and k' apply to every m in Fig. 3 (k and k' depend on the ATP cap, not on the length of the polymer), $kf_I = k'f_{II}$ (detailed balance). That is

$$\frac{k'}{k} = \frac{f_I}{f_{II}} = \frac{1 - p_0 - p_1 - p_2}{p_0 + p_1 + p_2} \tag{27}$$

$$= xK_1K_2c^2/(1 - x)\,\Sigma. \tag{28}$$

The two steady-state transition rates between states $N = 2$ and $N = 3$ in Fig. 1 *B* are also (by definition) the two steady-state rates between phases I and II. Furthermore, these two rates are equal, because of detailed balance. Thus, at steady state,

$$\text{Rate I} \rightarrow \text{II} = (k_{-3} + k_H)p_3 = kf_I \tag{29}$$

$$= \text{Rate II} \rightarrow \text{I} = k_3cp_2 = k'f_{II}. \tag{30}$$

From these relations we find

$$\begin{aligned} k &= (k_{-3} + k_H)\,(p_3/f_I) \\ &= (k_{-3} + k_H)\,(1 - x) = k_{-3} + k_H - k_3c, \end{aligned} \tag{31}$$

$$k' = k_3c(p_2/f_{II}) = k_3c \cdot K_1K_2c^2/\Sigma. \tag{32}$$

The quantities p_3/f_I and p_2/f_{II} are state probabilities within the separate phases. The form of k and k' is reminiscent of the Eyring rate theory. Note that Eqs. 31 and 32 are consistent with Eq. 28.

A representative part of the full kinetic diagram for an α end in which we follow both the cap size (N) and the gain or loss of subunits from the end (m) is shown in Fig. 4. Fig. 4 *A* indicates the possible transitions in and out of the various states m, N, and Fig. 4 *B* provides the corresponding rate constant labeling. Because every m level in Fig. 4 *A* has the same transitions and rate constants, the full two-dimensional diagram (Fig. 4 *A*) can be compressed vertically, without approximation, into the one dimensional diagram in Fig. 1 *B*. On the other hand, compression horizontally into the one-dimensional two-phase diagram in Fig. 3 (the I, II order is reversed) is, in general, *not* exact because the N values within each phase are not equivalent. However, the approximation will become very accurate if the two phases are cleanly separated, that is, if phase II is concentrated at $N = 0$ and if phase I is dominated by states with large N ($N \gg 3$). An equivalent definition of "clean separation" is that, when the two phases are about equally probable ($f_I \simeq 0.5$), there are, on the average, a large number of elementary transitions *within* each phase before a phase change occurs.

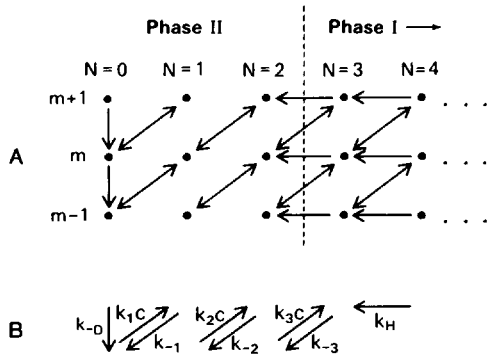

FIGURE 4 Kinetic diagram for the α end that is more detailed than either Fig. 1 *B* or Fig. 3 (i.e., both m and N are included).

Let us digress to be more explicit about the "not exact" comment above. Actually, *at steady state*, Eqs. 21–32 are formally exact by definition, whatever the choice of elementary rate constants in the model and whether or not there is clean separation between the two phases. However, to be useful and significant, a kinetic diagram like Fig. 3 must be valid not only at steady state but also in transients—e.g., any approach to steady state. However, Fig. 3 will be a good approximation to use for transients only if the elementary transitions *within* each phase are fast relative to transitions *between* phases so that each phase is practically in an internal steady state that is essentially unperturbed by the comparatively slow leakage between phases (i.e., phase changes). Thus, "not exact," above, refers to the general applicability of Fig. 3, not simply to steady states.

We denote the mean number of elementary transitions during the mean lifetime of phase I by T_I; T_{II} has a similar meaning for phase II. For any state ($N \geq 3$) in phase I, there are three possible elementary transitions: k_{-3}, k_3c, and k_H. The mean time $\bar{t}_I$ between transitions is then $(k_{-3} + k_3c + k_H)^{-1}$. The mean lifetime of phase I is k^{-1}. Hence, from Eq. 31,

$$T_I = (k_{-3} + k_H + k_3c)/(k_{-3} + k_H - k_{-3}c). \tag{33}$$

In phase II, states 0, 1, 2, have relative steady-state populations 1, K_1c, $K_1K_2c^2$ and mean times between transitions,

$$\begin{aligned} &\bar{t}_0 = (k_{-D} + k_1c)^{-1}, \quad \bar{t}_1 = (k_{-1} + k_2c)^{-1}, \\ &\bar{t}_2 = (k_{-2} + k_3c)^{-1}. \end{aligned} \tag{34}$$

Thus,

$$\bar{t}_{II} = (\bar{t}_0 + K_1c\bar{t}_1 + K_1K_2c^2\bar{t}_2)/\Sigma. \tag{35}$$

The mean lifetime of phase II is k'^{-1}. Hence

$$T_{II} = \Sigma/k'(\bar{t}_0 + K_1c\bar{t}_1 + K_1K_2c^2\bar{t}_2), \tag{36}$$

where k' is given in Eq. 32.

We now apply the above results to the actin case in Fig. 2. In addition to the parameters given following Eq. 18, we need k_1 and k_2, both of which we take as 1.7 $\mu M^{-1} s^{-1}$ (the same as for k_3; for example, the on rate constant is assumed to be diffusion controlled). Table I gives calculated values of k, k', f_I, T_I, and T_{II} at several concentrations below $c_0 = 11$ μM. The $f_I(c)$ curve is already included in Fig. 2. The values of T_I and T_{II} are all very small, except for the expected large T_I as $c \rightarrow c_0$ (the average cap is large and has a very long lifetime) and large T_{II} as $c \rightarrow 0$ (it requires a very long time for a cap to form, i.e., for the polymer to reach $N = 3$). At $f_I = f_{II} = 1/2$, neither "phase" survives for more than a few elementary transitions ($T_I \simeq 3$, $T_{II} \simeq 1$). Thus, judging from this example, actin does *not* show the dramatic phase-change behavior of microtubules (2–5), e.g, shortening to disappearance. The ATP cap has a profound effect on $J(c)$ and $J_H(c)$ in Fig. 2 [e.g., $J(c)$ is far from a simple linear curve, as for an equilibrium polymer] but this effect does *not* include alternating, long sessions in two different phases with quite different properties, as is the case for a microtubule end. In summary: for actin, the horizontal compression of the elementary kinetic diagram (Fig. 4) into the simpler two-phase diagram in Fig. 3 is inaccurate and not justified.

As a final topic, we examine an arbitrary and hypothetical special case of the model in Figs. 1 and 4 for which use of the two-phase diagram in Fig. 3 *is* appropriate. In this case we take

$$K_1 = 0.02\ \mu M^{-1}, \quad K_2 = K_3 = 0.2\ \mu M^{-1}, \quad k_H = 0,$$
$$k_1 = 0.1\ \mu M^{-1} s^{-1}, \quad k_2 = k_3 = 1\ \mu M^{-1} s^{-1},$$
$$k_{-1} = k_{-2} = k_{-3} = 5\ s^{-1}, \quad k_{-D} = 50\ s^{-1}. \qquad (37)$$

The main characteristics here are that the off rate constant (k_{-D}) for Ds is relatively large and that the attachment of a T onto the $N = 0$ (all D) state is relatively weak (K_1, k_1). Similar features are present at a microtubule end (2, 3); in the latter case (K_1, k_1), slow exchange of a GTP for GDP at position $n = 1$ is a possible alternative to GTP-tubulin attaching slowly to GDP-tubulin (i.e., the equivalent of the k_1 transition). We use $k_H = 0$ in Eqs. 37 to simplify the model without altering its essential properties (10). With the parameters in Eqs. 37, $c_\alpha = c_0 = 5$ μM. That is, the discontinuity in slope of $J(c)$ occurs at $J = 0$ (10).

TABLE I
"PHASE CHANGE" PROPERTIES FOR ACTIN

c	k	k'	f_I	T_I	T_{II}
μM	s^{-1}	s^{-1}			
0.10	18.53	0.028	0.0015	1.018	43.09
0.55	17.76	0.74	0.0400	1.105	1.644
2.50	14.45	4.11	0.2216	1.588	1.069
5.5364	9.29	9.29	0.5000	3.03	1.027
8.50	4.25	14.33	0.7713	7.80	1.017
10.50	0.85	17.73	0.9543	43.00	1.013

TABLE II
PHASE CHANGE PROPERTIES IN A SPECIAL CASE

c	k	k'	f_I	T_I	T_{II}
μM	s^{-1}	s^{-1}			
3.50	1.5000	0.1533	0.0927	5.67	215.62
4.20	0.8000	0.2567	0.2429	11.50	122.79
4.6575	0.3425	0.3425	0.5000	28.20	89.61
4.90	0.1000	0.3941	0.7976	99.00	76.88
4.96	0.0400	0.4076	0.9106	249.00	74.12
4.95236*	0.0476	0.0476	0.5000	208.9	974.6

*$K_1 = 0.002$, $k_1 = 0.01$.

Table II, for this case, corresponds to Table I for actin. The phase-change rate constants k and k' are much smaller in Table II than in Table I. Note that, in Table II, both T_I and T_{II} are moderately large on both sides of $f_I = f_{II} = 1/2$. Much larger values of T_I and T_{II} can be obtained simply by decreasing K_1 and k_1. For example, the last row in Table II refers to the case $K_1 = 0.002$ μM^{-1}, $k_1 = 0.01$ $\mu M^{-1} s^{-1}$ (with no change in other parameters), at $f_I = f_{II} = 1/2$. Because the T_I and T_{II} values in Table II are reasonably large, the two-phase approach in Eqs. 21–32 can be used as a good approximation in this example. This has been confirmed by a Monte Carlo simulation (courtesy of Dr. Yi-der Chen) at $c = 4.6575$ ($f_I = 1/2$), with averages printed every 10 transitions. There are clean phase changes and the phases occasionally survive for a large number of elementary transitions. For example, in the simulation of 50,000 transitions, lifetimes (in numbers of transitions) for phase I of 1230, 1120, 630, 500, 500, and 380 occurred (in Table II, the mean value is 28.2).

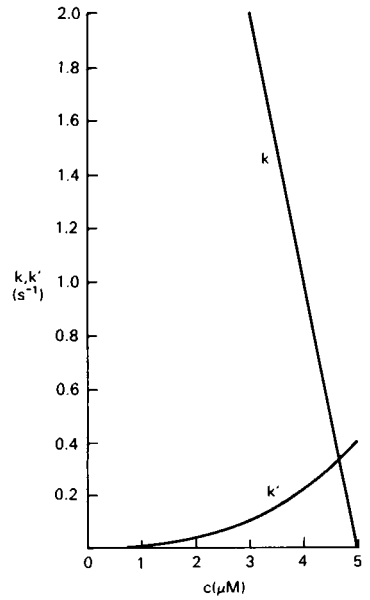

FIGURE 5 The phase-change rate constants $k(c)$ and $k'(c)$ for a hypothetical special case (Eqs. 37).

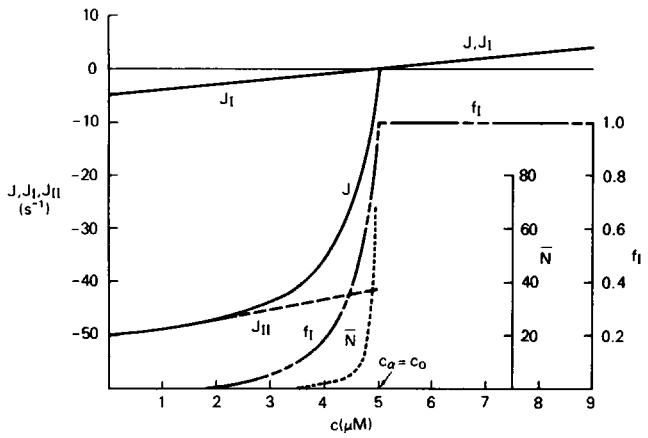

FIGURE 6 Further properties calculated for the same example as in Fig. 5. J_I and J_{II} are subunit fluxes in the two phases; J is a composite of J_I and J_{II} (Eq. 21).

Figs. 5 and 6 show several two-phase properties for this case (Eqs. 37). In Fig. 6, for $c < c_0$, $J(c)$ is an average between J_I and J_{II}, determined by f_I (Eq. 21). Phase I (cap) shortens slowly; phase II (no cap) shortens rapidly. The state of the polymer end jumps back and forth between the two phases, with rate constants $k(c)$ and $k'(c)$ shown in Fig. 5. As for a microtubule end (2, 3), the mean flux curve $J(c)$ in Fig. 6, for $c < c_0$, contains more than meets the eye: it is actually a composite of J_I and J_{II}. On the other hand, the actin $J(c)$ curve in Fig. 2, for $c < c_0$, has no such hidden components. The configurations at the end of an actin filament (judging from this model) do not alternate between two well-separated classes or phases. As a consequence, even though $J(c)$ is very nonlinear (Fig. 2) at both ends of an actin filament, owing to an ATP cap, the concept of treadmilling in an actin filament with two free ends retains its physical significance. However, in a microtubule, treadmilling is completely overshadowed by the extreme two-phase behavior occurring at both ends (9).

Received for publication 1 July 1985 and in final form 12 November 1985.

REFERENCES

1. Pantaloni, D., T. L. Hill, M. -F. Carlier, and E. D. Korn. 1985. A new model for actin polymerization and the kinetic effects of ATP hydrolysis. *Proc. Natl. Acad. Sci. USA.* 82:7207–7211.
2. Hill, T. L., and Y. Chen. 1984. Phase changes at the end of a microtubule with a GTP cap. *Proc. Natl. Acad. Sci. USA.* 81:5772–5776.
3. Chen, Y., and T. L. Hill. 1985. Monte Carlo study of the GTP cap in a five-start helix model of a microtubule. *Proc. Natl Acad. Sci. USA.* 82:1131–1135.
4. Mitchison, T., and M. W. Kirschner. 1984. Microtubule assembly nucleated by isolated centrosomes. *Nature (Lond.).* 312:232–237.
5. Mitchison, T., and M. W. Kirschner. 1984. Dynamic instability of microtubule growth. *Nature (Lond.).* 312:237–242.
6. Carlier, M. -F., T. L. Hill, and Y. Chen. 1984. Interference of GTP hydrolysis in the mechanism of microtubule assembly: an experimental study. *Proc. Natl. Acad. Sci. USA.* 81:771–775.
7. Hill, T. L. 1985. Cooperativity Theory in Biochemistry. Springer Verlag, New York.
8. Hill, T. L. 1984. Introductory analysis of the GTP-cap phase-change kinetics at the end of a microtubule. *Proc. Natl. Acad. Sci. USA.* 81:6728–6732.
9. Hill, T. L. 1985. Phase change kinetics for a microtubule with two free ends. *Proc. Natl. Acad. Sci. USA.* 82:431–436.
10. Hill, T. L., and M. -F. Carlier. 1983. Steady-state theory of the interference of GTP hydrolysis in the mechanism of microtubule assembly. *Proc. Natl. Acad. Sci. USA.* 80:7234–7238.